Polyesters with 1,4,7-trioxanonyl segments in their main chain. Novel ion-conducting matrices

J.J.A. Mertens[+], L.W. Jenneskens*[+], B.B. Wentzel[+], M. Wübbenhorst[++], J. van Turnhout[++] and R.H.M. van de Leur[+++]

[+] Debye Institute, Department of Physical Organic Chemistry, Utrecht University, Padualaan 8, 3584 CH Utrecht, The Netherlands
[++] Department of Polymer Science and Technology, Technical University Delft, Julianalaan 136, 2628 BL Delft, The Netherlands
[+++] TNO Plastics and Rubber Research Institute, P. O. Box 6031, 2600 JA Delft, The Netherlands

The amorphous polyester **1a** prepared by melt condensation of 1,5-*bis*-(9-hydroxy-1,4,7-trioxanonyl)naphthalene (**2a**) and adipoylchloride (**3a**), which contains *bis*-1,4,7-trioxanonyl (triethyleneglycol) segments in its main chain, represents a matrix for ion-conducting materials. Despite the fact that only triethyleneglycol segments are present, which are shorter than the minimum required for full solvation of Li^+ cations, ion-conductivities of $\sigma = 3.3 \times 10^{-5}$ S cm^{-1} at 368 K are found for Li^+/**1a** 0.25 (cations *per* polymer repeat unit). Hence, more than one *bis*-1,4,7-trioxanonyl segment (either intra- or interchain) has to be involved in Li^+ complexation. The σ value compares favorably with previous data for more complex polymer matrices.

1. Introduction

The development of processible solvent-free polymer electrolytes with ion-conductivities in the range $10^{-5}-10^{-2}$ S cm^{-1} at either ambient or elevated temperatures is a topical subject [1–3]. Suitable polymer matrices have to fullfil a number of requirements: 1) They have to solvate inorganic salts such as LiX and NaX with X being ClO_4^- or $CF_3SO_3^-$, which is achieved by incorporation of $-(CH_2CH_2X)_n-$ units [X being O, N and S] capable of coordinating these metal cations. 2) Since segmental motion of the polymer chains is a prerequisite for effective ion-transport, the polymer electrolytes have to be amorphous and preferably possess a low glass transition temperature (T_g). 3) They have to be both dimensionally as well as mechanically stable.

Taking into account these criteria poly(ethylene oxide) [PEO] was identified as an archetypal material [4, 5]. However, a drawback is the crystallinity of PEO and its salt/PEO complexes, which impairs ion-transport. To circumvent this problem PEO-derived co-polymers, networks and blends, as well as comb-branch polymers containing oligo(ethyleneglycol) side-chains and hyperbranched poly(ethyleneglycols) have been prepared and evaluated [1, 6–8].

Here we report the synthesis of a well-defined amorphous linear polyester (**1a**) obtained by melt condensation of 1,5-*bis*-(9-hydroxy-1,4,7-trioxanonyl)naphthalene (**2a**) and adipoylchloride (**3a**), which contains *bis*-1,4,7-trioxanonyl (triethyleneglycol) segments in its main chain. For solvent-free polymer electrolytes $LiClO_4$/**1a** ion-conductivities up to $\sigma = 3.3 \times 10^{-5}$ S cm^{-1} at 368 K are obtained. Since the *bis*-1,4,7-trioxanonyl segments are shorter than the minimum required for full solvation of a Li^+ cation, more than one segment (either intra- or interchain) has to be involved in Li^+ complexation. These results hold promise for the development of defined amorphous linear polyesters as well as crosslinked systems possessing higher σ values at even lower, viz. ambient, temperatures.

Fax: +31-302534533
e-mail: jennesk@chem.ruu.nl

2. Results and discussion

To establish the potential of linear polyesters with 1,4,7-trioxanonyl segments in their main chain for application as ionic conductors, polymers **1a–d** were prepared by melt condensation [9]. Diol monomers 1,5-*bis*-(9-hydroxy-1,4,7-trioxanonyl)naphthalene (**2a**) and 1,4-*bis*-(9-hydroxy-1,4,7-trioxanonyl)benzene (**2b**) were polymerized with either adipoylchloride (**3a**) or terephthaloylchloride (**3b**), respectively (Scheme 1). The high

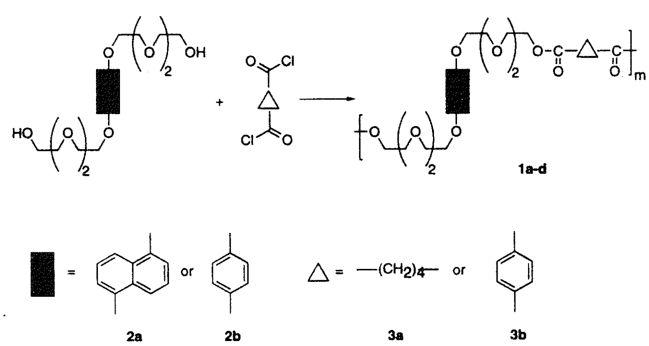

Scheme 1.

molecular weight fraction was separated from both linear and cyclic oligomers [10] by precipitation in CH_3OH and, if necessary, purified by reprecipitation (**1a–c**, highly viscous oils and **1d**, solid, Table 1). According to ^1H and ^{13}C-NMR as well as FT-IR spectroscopy endgroups were not discernible. Size exclusion chromatography (SEC) gave molecular weight distributions M_w ($D = M_w/M_n$) for **1a–d** in the range 1.6×10^4 (1.80) to 7.9×10^4 (2.56, Table 1) [11]. The thermal stability of **1a–d** was determined using thermogravimetry [TGA(N_2)]; no weight loss is found below 600 K. Wide angle X-ray diffraction (WAXD), polarization microscopy and differential scanning calorimetry (DSC) revealed that polyesters **1a–c** are amorphous materials with T_g (DSC) values below room temperature (Table 1). Polyester **1d**, by contrast, is *semi*-crystalline; discrete WAXD reflections ($d = 4.1, 3.9$ and 3.65 Å) as well as a T_g (DSC) of 244 K and a melt

Table 1. Selected data of polyesters **1a–d** prepared by melt condensation.

Polyesters	Monomers	Yield [%]	M_w [SEC]	D [M_w/M_n]	T_g [K] (T_{onset}/T_{offset})	TGA (N_2) [K] (T_{onset}/T_{max})[b]	$T_{(5\%\ weight\ loss)}$ [K]	$T_{(100\%\ weight\ loss)}$ [K]
1a	**2a/3a**	75	4.8×10^4	1.99	$T_g = 252.8$ (251/255)	598/683	637	900
1b	**2a/3b**	65	1.6×10^4	1.80	$T_g = 282.5$ (280/285)	608/713	664	1120
1c	**2b/3b**	58	2.2×10^4	1.89	$T_g = 267.2$ (266/269)	598/718	636	955
1d	**2b/3a**	40[a]	7.9×10^4	2.56	$T_g = 244$ (243/246) $T_m = 333$ [$\Delta H = 55$ Jg^{-1}]	608/695	655	865

[a] Reprecipitated twice in order to remove low molecular weight material.
[b] T_{max} taken from first derivative curve.

endotherm T_m (DSC) at 333 K with ΔH 55 J g^{-1} were found. As expected on the basis of the hydrocarbon architectures of the polyesters, the T_g (DSC) values increase in going from **1d**, **1a**, **1c** to **1b**, i.e. T_g (DSC) increases with increasing rigidity of especially the incorporated aromatic moieties.

To gain insight into the application of these linear polyesters as matrices for ion-conduction, solvent-free salt/polymer complexes, viz. polymer electrolytes, were prepared of **1a** and **b**, which differ only in the type of *bis*-acid chloride incorporated, via the following procedure. THF solutions of either polyester **1a** or **1b** and $LiClO_4$ were mixed followed by slow evaporation of the solvent under a N_2 atmosphere, giving highly viscous residues. To remove remaining traces of solvent the samples were dried in vacuo at 393 K. Salt/polymer complexes containing 0.125 to 1.0 Li^+ cations per polymer repeat unit, viz. the number of oxygen atoms per cation varies from 80 to 10, were obtained. WAXD and DSC showed that all solvent-free polymer electrolytes $LiClO_4$/**1a** and $LiClO_4$/**1b** are amorphous materials. In both series T_g (DSC) increases concomitantly with increasing Li^+ cation concentration. Linear relationships are found between the inverse of T_g (T_g^{-1}) and the Li^+ cation concentration expressed in mol dm^{-3} polymer (r^2; $LiClO_4$/**1a**, 0.96 and $LiClO_4$/**1b**, 0.95, Fig. 1). This indicates that the 1,4,7-trioxanonyl (triethyleneglycol) segments in the polymer main chain preferably form interchain, non-covalent physical (ion-dipole) crosslinks which will restrict segmental motions of the polymer. Since the slopes are similar ($LiClO_4$/**1a**, -2.80×10^{-4} dm^3 mol^{-1} K^{-1} and $LiClO_4$/**1b** -2.77×10^{-4} dm^3 mol^{-1} K^{-1}) [12] differences in hydrocarbon architecture of **1a** and **1b** derived from the monomers **2a** and **3a**, and **2a** and **3b**, respectively, appear not to affect Li^+ cation complexation. Moreover, the excellent agreement of the slopes with that found for isocyanate crosslinked PEO networks (-2.7×10^{-4} dm^3 mol^{-1} K^{-1}) [7] suggests that, independent of the polymer hydrocarbon architecture, the increase of T_g upon addition of Li^+ cations can be solely attributed to Li^+ cation complexation by the ethyleneglycol sequences present in the main chain.

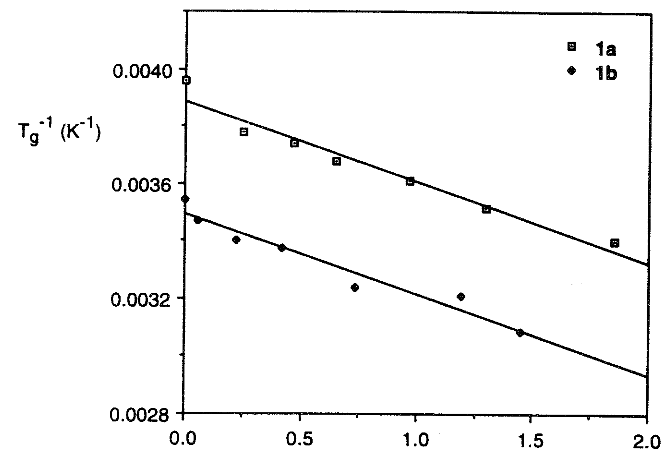

Fig. 1. Plot of T_g^{-1} for series $LiClO_4$/**1a** (▣) and $LiClO_4$/**1b** (◆) versus the amount of $LiClO_4$ expressed in mol dm^{-3} polymer [12].

Because polymer electrolytes $LiClO_4$/**1a** possess the lowest T_g values, their ion-conducting properties as a function of temperature and Li^+ cation concentration were assessed using AC impedance spectroscopy data (Experimental) [13]. With respect to pristine **1a**, incorporation of $LiClO_4$ leads to an increase of three orders of magnitude in ion-conductivity, i.e., from $\sigma = 2.6 \times 10^{-8}$ S cm^{-1} for **1a** to $\sigma = 3.3 \times 10^{-5}$ S cm^{-1} at 368 K for Li^+/**1a** 0.25. In contrast, all polymers containing Li^+ cations show at high temperatures (368 K) only a relatively small variation in σ (less than a factor 4). In fact the polymer electrolyte with a moderate concentation of Li^+ cations possesses the best ion-conducting properties (Fig. 2).

Nonetheless, the high temperature value $\sigma = 3.3 \times 10^{-5}$ S cm^{-1} at 368 K is comparable with values determined for PEO derived polymer electrolytes: $LiClO_4$/PEO (6×10^{-6} S cm^{-1} at 312 K) [14], NaI/PEO (10^{-6} S cm^{-1} at 298 K) [15], $LiClO_4$/oxymethylene linked PEO (5×10^{-5} S cm^{-1} at 298 K) [16], $LiClO_4$/PEO blends (10^{-5} S cm^{-1} at 298 K) [17] and $LiClO_4$/hyperbranched poly(ethyleneglycols) (10^{-5} S cm^{-1} at 303 K) [8].

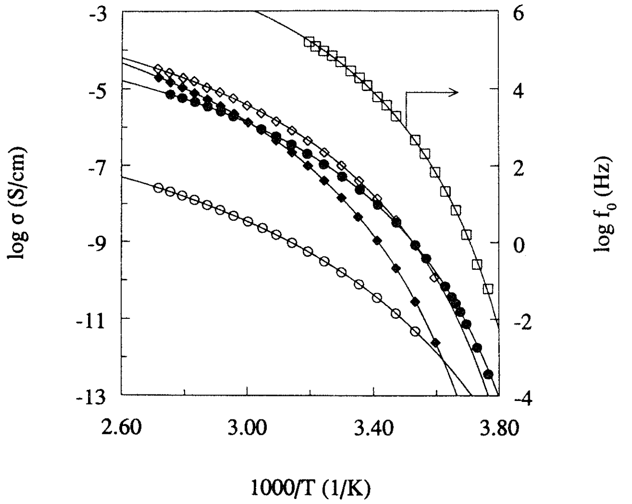

Fig. 2. Log σ vs. $1000/T$ for salt/polymer complexes $LiClO_4$/**1a**; (o) uncomplexed **1a**, (•) Li^+/**1a** 0.13, (◇) Li^+/**1a** 0.25, (◆) Li^+/**1a** 0.50; (□) Logf_0^a vs. $1000/T$ for Li^+/**1a** 0.13.

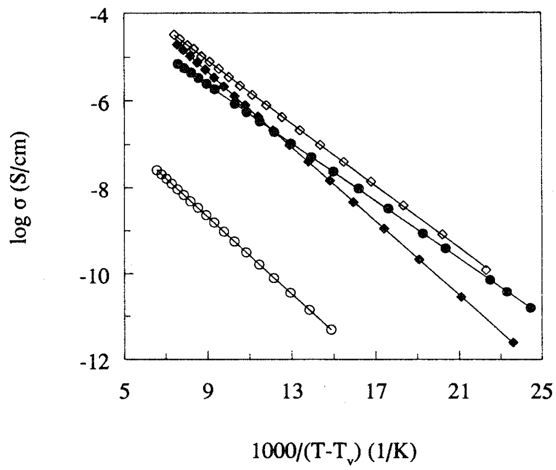

Fig. 3. Log σ vs. $1000/(T-T_v)$ for salt/polymer complexes $LiClO_4$/**1a**; (o) uncomplexed **1a**, (•) Li^+/**1a** 0.13, (◇) Li^+/**1a** 0.25, (◆) Li^+/**1a** 0.50.

The value of σ is markedly temperature dependent, albeit non-Arrhenius like, and was therefore analyzed using a Vogel-Fulcher-Tamman (VFT) [18] type equation (Eq. (1))

$$\sigma(T) = \sigma_\infty \exp\left(\frac{-E_v}{R(T-T_v)}\right) \quad (1)$$

in which R and T_v represent the gas constant [8.31 J mol^{-1} K^{-1}] and Vogel scaling temperature, while σ_∞ and E_v [kJ mol^{-1}] denote the ultimate conductivity and Vogel 'activation' energy. The fit results are shown in Fig. 2 (lines) as well as in Table 2. In order to enable a more convenient comparison of the conductivity curves the data are also presented as a function of the reduced temperature $T-T_v$ giving the linear graphs shown in Fig. 3. Although the absolute values of σ for polymer electrolytes $LiClO_4$/**1a** do not differ very much, an increasing temperature coefficient dlog/d$(1/(T-T_v)) \propto E_v$ with increasing Li^+ cation content is found.

As reported previously [19], the high accuracy of the VFT-fits in the temperature range $T_g < T < T_g + 100$ implies a strong interrelation of the ionic conductivity with the relaxation of the chain segments at and above the glass–rubber transition (α-relaxation, viz. glass transition temperature T_g). Further support for this conjunction was obtained by fitting the mean relaxation time τ_0 of the α-relaxation process taken from the dielectric loss peak with a VFT-equation $\ln\tau = \ln\tau_\infty - E_v/R(T-T_v)$. An example is presented in Fig. 2 for polymer electrolyte Li^+/**1a** 0.13. Indeed, the VFT-parameters (T_v and E_v) of both the dielectric relaxation rate (frequency $f_0 = 1/2\pi\tau_0$) and the conductivity compare very well. Only a slight divergence between $\log\sigma(T)$ and $\log f_0(T)$ occurs near T_g, which is expressed by a difference in T_v of ca. 5 K.

The observed strong coupling between segmental motion and ion-conduction can be rationalized in different ways. Considering that electrical conduction generally depends on the charge carrier concentration n_i, the charge q_i and the charge carrier mobility μ_i (Eq. (2)),

$$\sigma = \sum_i n_i q_i \mu_i \quad (2)$$

we conceive that the chain mobility might control either the generation (release of Li^+ cations) or the mobility μ_i of the charge carriers or both. Under the assumption that the charge carrier mobility μ_i is related to the free volume

Table 2. VFT and WLF fit parameters for Li^+/**1a** polymer electrolytes.

Sample	T_g DSC[a] [K]	VFT parameters $\log\sigma_\infty$	E_v [kJ mol^{-1}]	T_v [K]	WLF/free volume parameters $\log\sigma_{T_g}$	C_1	C_2 [K]	$f(T_g)$	$\alpha_f \times 10^4$ [K^{-1}]
Li^+/**1a** 0.00	253	–2.64	8.58	215.8	–14.64	12.0	37.2	0.036	9.7
Li^+/**1a** 0.13	265	–0.61	6.41	231.1	–10.5	9.9	33.9	0.044	12.9
Li^+/**1a** 0.25	268	0.18	6.90	233.4	–10.22	10.4	34.6	0.042	12.1
Li^+/**1a** 0.50	277	0.55	8.25	235.6	–9.85	10.4	41.4	0.042	10.1
Li^+/**1a** 0.13	265		6.0[b]	236[b]		10.7	29		

[a] T_g DSC was also determined for Li^+/**1a** 0.33 (272 K) Li^+/**1a** 0.67 (285 K) and Li^+/**1a** 1.00 (294 K) [see Fig. 1].
[b] VFT parameters determined from the α-peak (see text).

[20], the temperature dependence $\sigma(T)$ can be described by the William–Landel–Ferry (WLF) [21] equation (Eq. (3))

$$\log\left(\frac{\sigma(T)}{\sigma_{T_g}}\right) = \frac{C_1(T - T_g)}{C_2 + T - T_g} \tag{3}$$

in which $C_1 = 17.4$ and $C_2 = 51.6$ K represent 'universal' constants for amorphous polymers. T_g is the dilatometric glass transition temperature ($\approx T_g$ (DSC)) and σ_{T_g} denotes the conductivity at T_g. Note that Eqs. (1) and (3) are essentially equivalent and can be transformed into each other using the relations $C_2 = T_g - T_v$, $C_1 = E_v/(2.30R\,C_2)$ and $\log\sigma_{T_g} = \log\sigma_\infty - C_1$ [22].

The WLF parameters C_1 and C_2 can be related directly to quantities resulting from the free volume concept by the expressions $f(T_g) = b/(\ln 10\ C_1)$ and $\alpha_f = f(T_g)/C_2$, where $f(T_g)$ and α_f denote the fractional free volume at T_g and its temperature coefficient; b is a constant. With $b = 1$ [20, 21], α_f and $f(T_g)$ were calculated. The results are given in Table 2 and show a significantly higher fractional free volume at T_g for the polymer electrolytes containing Li^+ cations. This can be likely attributed to the occurrence of non-covalent physical (ion-dipole) crosslinking. It is noteworthy that also pristine **1a** exhibits an $f(T_g)$ value of 0.036, which is higher than that predicted using the 'universal' constants [$f(T_g)$ 0.025]. The behavior of α_f will be discussed in detail in combination with a comprehensive analysis of dipolar relaxation phenomena in a forthcoming paper [23].

It seems plausible that Li^+ cation complexation will be affected by changes in segmental motion of the polymer chains. Consequently, the concentration of mobile Li^+ cations might vary. Our observation that for increasing Li^+ cation contents, viz. Li^+/**1a** > 0.25, σ does not increase anymore, suggests that the mobility μ_i of the Li^+ cations is hindered by reduction of the number and length of flexible ethyleneglycol sequences due to (temporary) physical crosslinking (Fig. 2).

3. Conclusions

The readily accessible, amorphous polyester **1a**, which contains *bis*-1,4,7-trioxanonyl (triethyleneglycol) segments in its main chain, represents a matrix for ion-conducting materials. Despite the fact that only triethyleneglycol segments are present, which are shorter than the minimum required for full solvation of Li^+ cations, ion-conductivities of $\sigma = 3.3 \times 10^{-5}$ S cm^{-1} at 368 K are found for Li^+/**1a** 0.25 (cations per polymer repeat unit). Hence, more than one *bis*-1,4,7-trioxanonyl segment (either intra- or interchain) has to be involved in Li^+ complexation. The σ value compares favorably with previous data for more complex polymer matrices. The results hold promise for the development of defined linear polyesters as well as crosslinked systems possessing higher σ values at even lower, viz. ambient, temperatures.

4. Experimental

4.1. Monomer synthesis

1,5-*Bis*-(9-hydroxy-1,4,7-trioxanonyl)naphthalene (**2a**) and 1,4-*bis*-(9-hydroxy-1,4-7-trioxanonyl)benzene (**2b**) were synthesized by etherification of 1,5-*bis*hydroxynaphthalene and 1,4-*bis*hydroxybenzene, respectively, with 2 equiv. 2-[2-(2-chloroethoxy)ethoxy]ethanol with potassium carbonate as base using available literature procedures [24, 25]. The analytical data of **2a** and **2b** were in full agreement with those reported earlier.

4.2. Melt polycondensation

The different combinations of the diols **2a–b** (5 mmol) and *bis*-acid chlorides **3a–b** (5 mmol) were mixed in a Schlenk apparatus under a dry N_2 atmosphere and, subsequently, heated to 373 K under continuous evacuation to remove evolved HCl(g). After ca. 20 min the reaction mixture became too viscous to enable magnetic stirring. Therefore, the temperature was raised to 453 K for 20 min to force polycondensation to completion. After cooling the reaction mixture was dissolved in THF (30 ml) and precipitated in vigorously stirred CH_3OH (180 ml) (Scheme 1). NMR spectra were recorded on a Bruker AC 300 spectrometer at 300.13 (^{1}H) and 75.47 (^{13}C) MHz using the solvent as internal standard. Molecular weight distributions were determined with size exclusion chromatography (Thermo Separation Products Spectra Series P200, Shodex Standard KF-804 column, eluent THF, UV detection (λ = 254 nm), reference polystyrene standards). Thermal properties were determined with differential scanning calorimetry (Mettler DSC 12-E, temperature range 233–473 K; heating and cooling rate 5 K min^{-1} and 2 K min^{-1}, respectively) and thermogravimetry (TGA (N_2), Perkin Elmer TGS-2 with an autobalance AR-2, temperature range 323–1123 K, heating rate 20 K min^{-1}). Dielectric measurements were performed on dried samples with AC impedance spectroscopy (Solartron 1250/1260 Frequency Response Analyzer for frequencies up to 1 kHz and a Hewlett-Packard 4284A LCR Meter for frequencies between 1 kHz and 1 MHz) by using parallel plates as well as a comb-like electrode geometry on a glass plate [26]. To circumvent resistance to ion flow at the electrode–electrolyte interface a sinusoidal voltage was applied to the system. Ion-conductivities σ (S cm^{-1}) were determined by fitting of up to two relaxation functions and a (ohmic) conduction term to the complex permittivity ε^* measured in the frequency range from 0.1 Hz to 100 kHz.

1a (from **2a** and **3a**): ^{1}H NMR ($CDCl_3$): δ 7.85 (d, 2H, ^3J = 8.5 Hz), 7.33 (dd, 2H, ^3J = 8.5 Hz and ^3J = 7.6 Hz), 6.83 (d, 2H, ^3J = 7.6 Hz), 4.29–4.26 (m, 4H), 4.23–4.20 (m, 4H), 3.99–3.94 (m, 4H), 3.80–3.77 (m, 4H), 3.72–3.66 (m, 8H), 2.32–2.28 (m, 4H), 1.65–1.60 (m, 4H) ppm; ^{13}C NMR ($CDCl_3$): δ 173.1, 154.3, 126.8, 125.1, 114.6, 105.7, 70.9, 70.6, 69.8, 69.2, 67.9, 63.4, 33.7 and 24.2 ppm; IR(KBr) 3060, 2947, 2883, 1741, 1273, 1143 and 787 cm^{-1} (see also Table 1 and Scheme 1);

Anal. Calcd for $(C_{28}H_{38}O_{10})_n$: C, 62.91; H, 7.17. Found: C, 62.84; H, 7.13.

1b (from **2a** and **3b**): ^{1}H NMR ($CDCl_3$): δ 8.07 (s, 4H), 7.83 (d, 2H, $^3J = 8.5$ Hz), 7.31 (dd, 2H, $^3J = 8.5$ Hz and $^3J = 7.6$ Hz), 6.79 (d, 2H, $^3J = 7.6$ Hz), 4.49–4.46 (m, 4H), 4.27–4.24 (m, 4H), 3.99–3.96 (m, 4H), 3.86–3.72 (m, 12H) ppm; ^{13}C NMR ($CDCl_3$): δ 165.7, 154.3, 133.9, 129.6, 126.7, 125.0, 114.6, 105.6, 71.0, 70.7, 69.8, 69.1, 67.8 and 64.4 ppm; IR(KBr) 3088, 2893, 1728, 1278, 1111 and 787 cm^{-1} (see also Table 1 and Scheme 1); Anal. Calcd for $(C_{30}H_{34}O_{10})_n$: C, 64.97; H, 6.18. Found: C, 64.85; H, 6.20.

1c (from **2b** and **3b**): ^{1}H NMR ($CDCl_3$): δ 8.10 (s, 4H), 6.81 (s, 4H), 4.51–4.48 (m, 4H), 4.06–4.03 (m, 4H), 3.87–3.80 (m, 8H), 3.77–3.73 (m, 8H) ppm; ^{13}C NMR ($CDCl_3$): δ 165.6, 153.0, 133.9, 129.6, 115.4, 70.7, 70.6, 69.9, 69.1, 67.9 and 64.4 ppm; IR(KBr) 3065, 2940, 2890, 1732, 1280, 1120 and 730 cm^{-1} (see also Table 1 and Scheme 1).

1d (from **2b** and **3a**): ^{1}H NMR ($CDCl_3$): δ 6.83 (s, 4H), 4.24–4.20 (m, 4H), 4.08–4.05 (m, 4H), 3.84–3.80 (m, 4H), 3.71–3.68 (m, 12H), 2.34 (m, 4H), 1.67–1.64 (m, 4H) ppm; ^{13}C NMR (DMSO-d_6): δ 172.5, 152.4, 115.2, 69.7, 69.6, 68.9, 68.2, 67.4, 62.9, 32.9 and 23.7 ppm; IR(KBr) 3051, 2918, 2870, 1734, 1242, 1118 and 780 cm^{-1} (see also Table 1 and Scheme 1).

References

[1] M.A. Ratner, D.F. Shriver, *Chem. Rev.* **1988**, *88*, 109.
[2] K. Murata, *Electrochim. Acta* **1995**, *13–14*, 2177.
[3] M. Andrei, A. Roggero, L. Marchese, S. Passerini, *Polymer* **1994**, *35*, 3592.
[4] D.E. Fenton, J.M. Parker, P.V. Wright, *Polymer* **1973**, *14*, 589.
[5] M.B. Armand, J.M. Chabagno, M.J. Duclot, in *Fast Ion Transport in Solids* (Eds: P. Vashishta, J.N. Mundy, G.K. Shenoy), North-Holland, Amsterdam **1979**, p. 131.
[6] Z. Florjanczyk, W. Krawiec, W. Wieczorek, M. Siekierski, *J. Polym. Sci. B* **1995**, *33*, 629.
[7] J.-F. Le Nest, A. Gandini, H. Cheradame, *Br. Polym. J.* **1988**, *20*, 253; J.-F. Le Nest, A. Gandini, H. Cheradame, J.-P. Cohen-Addad, *Macromolecules* **1988**, *21*, 1117.
[8] C.J. Hawker, F. Chu, P.J. Pomery, D.J.T. Hill, *Macromolecules* **1996**, *29*, 3831.
[9] M. Ballauf, *Makromol. Chem., Rapid Commun.* **1986**, *7*, 407.
[10] I.J.A. Mertens, L.W. Jenneskens, E.J. Vlietstra, A.C. van der Kerk-van Hoof, J.W. Zwikker, W.J.J. Smeets, A.L. Spek, *J. Chem. Soc., Chem. Commun.* **1995**, 1621.
[11] M. Ignatova, N. Manolova, I. Rashkov, *Macromol. Chem. Phys.* **1995**, *196*, 2695.
[12] Slopes of -2.80×10^{-4} dm^3 mol^{-1} K^{-1} and -2.77×10^{-4} dm^3 mol^{-1} K^{-1} were obtained under the assumption that the density (d) of polymers **1a–b** is 1 kg dm^{-3}. With either $d = 0.9$ or 1.1 kg dm^{-3} the slopes are -3.11×10^{-4} dm^3 mol^{-1} K^{-1} and -3.10×10^{-4} dm^3 mol^{-1} K^{-1}, and, 2.54×10^{-4} dm^3 mol^{-1} K^{-1} and -2.53×10^{-4} dm^3 mol^{-1} K^{-1}, respectively.
[13] J.R. MacDonald, *Impedance Spectroscopy: Emphasizing Solid Materials and Systems*, **1987**, Wiley, New York.
[14] D.J. Bannister, G.R. Davies, I.M. Ward, J.E. McIntyre, *Polymer* **1984**, *25*, 1600.
[15] P. Manoravi, I.I. Selvaraj, V. Chandrasekhar, K. Shahi, *Polymer* **1993**, *34*, 1339.
[16] C.V. Nicholas, D.J. Wilson, C. Booth, J.R.M. Giles, *Br. Polym. J.* **1988**, *20*, 289.
[17] W. Wieczorek, A. Zalewska, D. Raducha, Z. Florjanczyk, J.R. Stevens, A. Ferry, P. Jacobsson, *Macromolecules* **1996**, *29*, 143.
[18] H. Vogel, *Z. Phys.* **1921**, *22*, 645; G. Tamman, G. Hesse, *Z. Anorg. Allg. Chem.* **1926**, *156*, 245; G.S. Fulcher, *J. Am. Ceram. Soc.* **1971**, *54*, 591.
[19] T. Miyamoto, K. Shibayama, *J. Appl. Phys.* **1973**, *44*, 5372.
[20] A.K. Doolittle, *J. Appl. Phys.* **1951**, *22*, 1471; **1952**, *23*, 236.
[21] M.L. Williams, R.F. Landel, J.D. Ferry, *J. Am. Chem. Soc.* **1955**, *77*, 3701.
[22] For a review see: M.A. Ratner, *Polymer Electrolytes Reviews-1* (Eds: J.R. Callum, C.A. Vincent), Elsevier Applied Science, London **1987**, p. 173.
[23] I.J.A. Mertens, M. Wübbenhorst, L.W. Jenneskens, W. Oosterbaan, B. B. Wentzel, J. van Turnhout, unpublished.
[24] M.J. Gunter, D.C.R. Hockless, M.R. Johnston, B.W. Skelton, A.H. White, *J. Am. Chem. Soc.* **1994**, *116*, 4810.
[25] P.L. Anelli, P.R. Ashton, N. Spencer, A.M.Z. Slawin, J.F. Stoddart, D.J. Williams, *Angew. Chem., Int. Ed. Engl.* **1991**, *30*, 1036.
[26] H.W.L. Bruckman, M.P. de Goeje, *Prog. Org. Coatings* **1992**, *20*, 501.

Received April 17, 1997